Mechanistic Implications of Proton Transfer Coupled to Electron Transfer

Estelle L. Lebeau,[†] Robert A. Binstead,[§] and Thomas J. Meyer*[,‡]

Contribution from the Los Alamos National Laboratory, Associate Laboratory Director for Strategic and Supporting Research, MS A127, Los Alamos, New Mexico 87545, Department of Chemistry, University of North Carolina at Chapel Hill, Chapel Hill, North Carolina 27599-3290, and Department of Chemistry, 268 Dow Science Complex, Central Michigan University, Mount Pleasant, Michigan 48859

Received February 11, 2000

Abstract: The kinetics of electron transfer for the reactions *cis*-$[Ru^{IV}(bpy)_2(py)(O)]^{2+}$ + H^+ + $[Os^{II}(bpy)_3]^{2+}$ ⇌ *cis*-$[Ru^{III}(bpy)_2(py)(OH)]^{2+}$ + $[Os^{III}(bpy)_3]^{3+}$ and *cis*-$[Ru^{III}(bpy)_2(py)(OH)]^{2+}$ + H^+ + $[Os^{II}(bpy)_3]^{2+}$ ⇌ *cis*-$[Ru^{II}(bpy)_2(py)(H_2O)]^{2+}$ + $[Os^{III}(bpy)_3]^{3+}$ have been studied in both directions by varying the pH from 1 to 8. The kinetics are complex but can be fit to a double "square scheme" involving stepwise electron and proton transfer by including the disproportionation equilibrium, 2*cis*-$[Ru^{III}(bpy)_2(py)(OH)]^{2+}$ ⇌ (3×10^3 M^{-1} s^{-1} forward, 2.1×10^5 M^{-1} s^{-1} reverse) *cis*-$[Ru^{IV}(bpy)_2(py)(O)]^{2+}$ + *cis*-$[Ru^{II}(bpy)_2(py)(H_2O)]^{2+}$. Electron transfer is outer-sphere and uncoupled from proton transfer. The kinetic study has revealed (1) pH-dependent reactions where the pH dependence arises from the distribution between acid and base forms and not from variations in the driving force; (2) competing pathways involving initial electron transfer or initial proton transfer whose relative importance depends on pH; (3) a significant inhibition to outer-sphere electron transfer for the Ru^{IV}═O^{2+}/Ru^{III}—OH^{2+} couple because of the large difference in pK_a values between Ru^{IV}═OH^{3+} (pK_a < 0) and Ru^{III}—OH^{2+} (pK_a > 14); and (4) regions where proton loss from *cis*-$[Ru^{II}(bpy)_2(py)(H_2O)]^{2+}$ or *cis*-$[Ru^{III}(bpy)_2(py)(OH)]^{2+}$ is rate limiting. The difference in pK_a values favors more complex pathways such as proton-coupled electron transfer.

Introduction

Oxidation−reduction reactions in which there is a two-electron change, but which occur in one-electron steps, are often slow because of the intervention of unstable radicals.[1−3] The examples in Scheme 1 show that oxidation of methanol to formaldehyde is accessible to many chemical oxidants but that if $^{\bullet}CH_2OH$ is involved as an intermediate, the driving force required is increased by 1.5 V. Similarly, one-electron reduction of CO_2 to $^{\bullet}CO_2H$ requires a driving force more negative than that for two-electron reduction to HCO_2H by 2.0 V.

For mechanisms involving electron transfer, this greatly increases the magnitude of the free energy barrier, ΔG^*. From Marcus−Hush theory, ΔG^* increases quadratically with the free energy change, $\Delta G°$, as shown in eq 1 with λ the sum of the intramolecular and solvent reorganizational energies.[4−6]

$$\Delta G^* = (\lambda + \Delta G°)^2/4\lambda \qquad (1)$$

This is a generally recognized phenomenon for reactions involving unstable organic, inorganic, and biological radicals.[7−9]

Scheme 1[a]

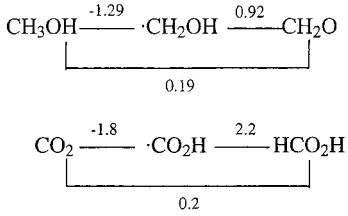

[a] $E°$ in V vs NHE. Sources: Endicott, J. F. In *Concepts of Inorganic Photochemistry*; Adamson, A. W., Fleischauer, P. D., Eds.; Wiley: New York, 1975; Chapter 3. Taylor, S. M.; Halpern, J. *Faraday Soc. Discuss.* **1960**, *29,* 174-181.

A related phenomenon exists for one-electron transfer, where there is a change in acidity upon oxidation or reduction.[10,11] In the inorganic example in Scheme 2, oxidation of Ru^{II} to Ru^{III} decreases the pK_a for bound H_2O by 9.7 pK_a units. At pH 7, the thermodynamic potential for oxidation of *cis*-$[Ru^{II}(bpy)_2(py)(H_2O)]^{2+}$ (bpy = 2,2′-bipyridine, py = pyridine) to *cis*-$[Ru^{III}(bpy)_2(py)(OH)]^{2+}$ is 0.66 V vs NHE. If the mechanism involves initial electron transfer to give *cis*-$[Ru^{III}(bpy)_2(py)(H_2O)]^{3+}$, 1.04 V is required. The thermodynamic potential for oxidation of *cis*-$[Ru^{III}(bpy)_2(py)(OH)]^{2+}$ to

* Address correspondence to this author: Associate Laboratory Director for Strategic and Supporting Research, Los Alamos National Laboratory, MS A127, Los Alamos, NM 87545.
‡ Los Alamos National Laboratory.
§ University of North Carolina at Chapel Hill.
† Central Michigan University.

(1) *Photoinduced Electron Transfer*; Fox, M. A., Chanon, M., Eds.; Elsevier: New York, 1998.
(2) *Electron-Transfer Reactions in Organic Chemistry*; Eberson, L. E., Ed.; Springer-Verlag: New York, 1987.
(3) Ashby, E. C. *Acc. Chem. Res.* **1980**, *21,* 414.
(4) Newton, M. D.; Sutin, N. *Annu. Rev. Phys. Chem.* **1984**, *35*, 437.
(5) Marcus, R. A. *Rev. Mod. Phys.* **1993**, *63*, 599.
(6) Marcus, R. A.; Sutin, N. *Biochim. Biophys. Acta* **1985**, *811*, 265.
(7) *Energetics of organic free radicals*; Simões, J. A. M., Greenberg, A., Liebman, J. F., Eds.; Blackie Academic & Professional: New York, 1996.
(8) *Radical Chemistry*; Perkins, M. J., Ed.; Ellis Horwood: New York, 1994.
(9) Barbara, P. F.; Meyer, T. J.; Ratner, M. A. *J. Phys. Chem.* **1996**, *100,* 13148−13168.
(10) Laviron, E. *J. Electroanal. Chem. Soc.* **1986**, *208*, 357.
(11) Kim, J.; Sistare, M. F.; Carter, P. J.; Thorp, H. H. *Coord. Chem. Rev.* **1998**, *171*, 341.

10.1021/ja000517a CCC: $20.00
Published on Web 10/04/2001

Scheme 2[a]

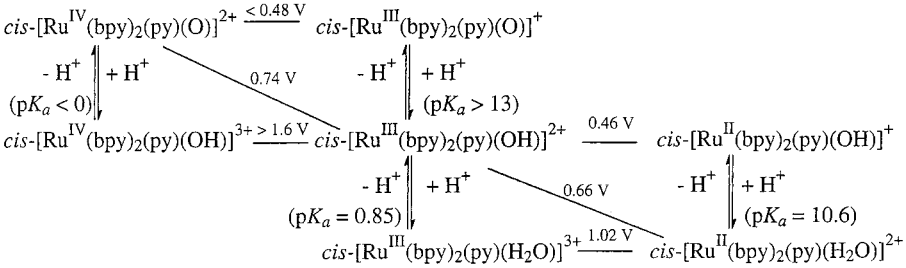

[a] In V vs NHE, pH 7, 25 °C, $I = 0.1$ M.

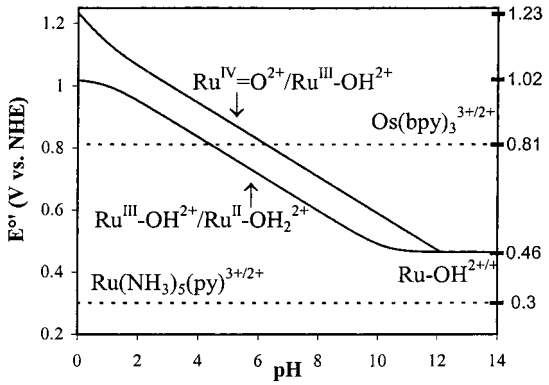

Figure 1. pH dependences for the couples *cis*-$[Ru^{IV}(bpy)_2(py)(O)]^{2+}$/*cis*-$[Ru^{III}(bpy)_2(py)(OH)]^{2+}$ (Ru^{IV}═O^{2+}/Ru^{III}—OH^{2+}) and *cis*-$[Ru^{III}(bpy)_2(py)(OH)]^{2+}$/*cis*-$[Ru^{II}(bpy)_2(py)(OH_2)]^{2+}$ (Ru^{III}—OH^{2+}/Ru^{II}—OH_2^{2+}) (vs NHE, 25 °C, $\mu = 0.1$ M). The potentials for the pH-independent $[Ru(NH_3)_5(py)]^{3+/2+}$ and $[Os(bpy)_3]^{2+/3+}$ couples are also shown.

cis-$[Ru^{IV}(bpy)_2(py)(O)]^{2+}$ is 0.74 V, but initial oxidation to *cis*-$[Ru^{IV}(bpy)_2(py)(OH)]^{3+}$ requires >1.6 V. [12,13]

In this article, we explore the kinetic nuances and mechanistic implications of outer-sphere electron-transfer reactions in which there are changes in proton content. The study was based on the reactions between the couples in Scheme 2 and the couples $[Os(bpy)_3]^{3+/2+}$ and $[Ru(NH_3)_5(py)]^{3+/2+}$.[14,15] The $Os^{III/II}$ couple is especially appropriate because its potential is near those for the Ru couples, but independent of pH. As illustrated by the pH dependences of the couples in Figure 1, its reactions can be investigated in either direction by varying the pH.

The following abbreviations will be used throughout:

$$Ru^{IV}{=}O^{2+} = \textit{cis}\text{-}[Ru^{IV}(bpy)_2(py)(O)]^{2+}$$

$$Ru^{III}{-}OH^{2+} = \textit{cis}\text{-}[Ru^{III}(bpy)_2(py)(OH)]^{2+}$$

$$Ru^{III}{-}OH_2^{3+} = \textit{cis}\text{-}[Ru^{III}(bpy)_2(py)(H_2O)]^{3+}$$

$$Ru^{II}{-}OH^{+} = \textit{cis}\text{-}[Ru^{II}(bpy)_2(py)(OH)]^{+}$$

$$Ru^{II}{-}OH_2^{2+} = \textit{cis}\text{-}[Ru^{II}(bpy)_2(py)(H_2O)]^{2+}$$

Experimental Section

Materials. High-purity deionized water was obtained by passing distilled water through a Nanopure (Barnstead) water purification system. Sodium phosphate monobasic monohydrate, $NaH_2PO_4{\cdot}H_2O$, sodium phosphate dibasic heptahydrate, $Na_2HPO_4{\cdot}7H_2O$, sodium phosphate tribasic dodecahydrate, $Na_3PO_4{\cdot}12H_2O$, and phosphoric acid, H_3PO_4, were obtained from Fisher Scientific and used without further purification in the preparation of buffer solutions. All other materials were reagent grade and used without additional purification. The salts *cis*-$[Ru^{II}(bpy)_2(py)(H_2O)](ClO_4)_2$, *cis*-$[Ru^{III}(bpy)_2(py)(OH)](ClO_4)_2$, *cis*-$[Ru^{IV}(bpy)_2(py)(O)](ClO_4)_2$, $[Os^{II}(bpy)_3](PF_6)_2$, $[Os^{III}(bpy)_3](PF_6)_3$, and $[Os^{II}(bpy)_2(4\text{-}CO_2H\text{-}4'\text{-}CH_3bpy)](PF_6)_2$ {4-CO_2H-4′-CH_3-bpy = 4′-methyl-2,2′-bipyridine-4-carboxylic acid} were all prepared according to previously reported methods.[16−19]

Instrumentation. Routine UV−visible spectra were recorded on a Hewlett-Packard 8452A diode array spectrophotometer in standard quartz cells. Kinetic measurements were carried out on a Hi-Tech Scientific SF-61MX stopped-flow multimixing spectrophotometer. The temperature of the reactant solutions was controlled to within ±0.02 °C by using a Neslab RTE-110 water bath circulator. The pH of solutions used for kinetics measurements was determined by using a Radiometer model 62 pH meter and a Ross model 81-02 combination electrode after calibration with standard buffer solutions.

Kinetic Measurements. Rate data in water were collected by following visible spectral changes at a series of pH values. Wavelengths were chosen where large spectral changes were observed or where component absorbances could be isolated. These included isosbestic points—345 and 445 nm (Ru^{IV}═O^{2+} and Ru^{III}—OH^{2+}), 400 nm (Ru^{II}—OH_2^{2+} and Ru^{III}—OH^{2+}), and 450 nm (Ru^{II}—OH_2^{2+} and Os^{II})—and 472 and 630 nm where Ru^{II}—OH_2^{2+} or Os^{II}, respectively, dominates absorbance changes. In the complete study, greater than 500 separate kinetic traces were collected on approximately 60 separate solutions at a series of pH values from pH 0.6 to 8.3.

In the stopped-flow experiments, data were acquired at single wavelengths because measurements in the diode array configuration were complicated by photochemical processes. They included photoreduction of Ru^{IV}═O^{2+} and Ru^{III}—OH^{2+} and pyridine photolabilization from Ru^{II}—OH_2^{2+}.

Triple mixing was employed at basic pH values (pH > 6) because of the instability of $[Os^{III}(bpy)_3]^{3+}$ for extended periods under these conditions. The instability arises from self-reduction by ligand oxidation as the pH is increased, as has been reported for many pyridyl and polypyridyl complexes, including $[Ru^{III}(bpy)_3]^{3+}$ and $[Fe^{III}(bpy)_3]^{3+}$.[20−22] Creutz and Sutin[20] describe the kinetics of decomposition of $[Ru^{III}(bpy)_3]^{3+}$ in basic media as dominated by rate-determining nucleophilic attack by hydroxide on the bound bypyridine ligand. The pH jump experiments minimize complications from decomposition of $[Os^{III}(bpy)_3]^{3+}$.

(12) Binstead, R. A.; McGuire, M. E.; Dovletoglou, A.; Seok, W. K., Roecker, L. E.; Meyer, T. J. *J. Am. Chem. Soc.* **1992**, *114*, 173−186.
(13) Trammell, S. A.; Wimbish, J. C.; Odobel, F.; Gallagher, L. A.; Narula, P. M.; Meyer, T. J. *J. Am. Chem. Soc.* **1998**, *120*, 13248−13249.
(14) Braddock, J. L.; Cramer, J. L.; Meyer, T. J. *J. Am. Chem. Soc.* **1975**, *97*, 1972.
(15) Chou, M.; Creutz, C.; Sutin, N. *J. Am. Chem. Soc.* **1977**, *96*, 5615.
(16) Moyer, B. A.; Meyer, T. J. *Inorg. Chem.* **1981**, *20*, 436−444.
(17) Sullivan, B. P.; Salmon, D. J.; Meyer, T. J. *Inorg. Chem.* **1978**, *17*, 3334−3341.
(18) Kober, E. M.; Caspar, J. V.; Sullivan, B. P.; Meyer, T. J. *Inorg. Chem.* **1988**, *27*, 4587−4598.
(19) Dupray, L. M.; Meyer, T. J. *Inorg. Chem.*, **1996**, *35*, 6299−6307.
(20) Creutz, C.; Sutin, N. *Proc. Natl. Acad. Sci. U.S.A.* **1975**, *72*, 2858−2862.
(21) Roecker, L. R.; Kutner, W.; Gilbert, J. A.; Simmons, M.; Murray, R. W.; Meyer, T. J. *Inorg. Chem.* **1985**, *24*, 3284.
(22) Nord, G.; Pedersen, B.; Bjergbakke, E. *J. Am. Chem. Soc.* **1983**, *105*, 1913−1919.

In the kinetic experiments, the initial concentrations of $Ru^{IV}{=}O^{2+}$ or $Ru^{III}{-}OH^{2+}$ were varied from 1×10^{-7} to 2×10^{-4} M and those of $[Os^{II}(bpy)_3]^{2+}$ and $[Os^{III}(bpy)_3]^{3+}$ from 8×10^{-7} to 2×10^{-4} M. The temperature was maintained at 25 ± 0.1 °C. The buffers used were H_3PO_4 and $NaH_2PO_4{\cdot}H_2O$ below pH 4, $NaH_2PO_4{\cdot}H_2O$ and $Na_2HPO_4{\cdot}7H_2O$ between pH 4 and 9, and $Na_2HPO_4{\cdot}7H_2O$ and $Na_3PO_4{\cdot}12H_2O$ for pH > 9. Ionic strength was maintained at 0.1 M. The reactions were carried out under pseudo-first-order conditions with the reductant in excess and the reactants at equal concentrations, or under pseudo-first-order conditions with the oxidant in excess.

Kinetic Analysis. All manipulations of spectral data were performed by using SPECFIT (Spectrum Software Associates, Chapel Hill, NC) software. This program allows for a global fit of absorbance/time data to a user input model, see below.

Results

To understand the logic behind the design of the kinetics experiments, it is useful to refer to the potential−pH diagram in Figure 1. This diagram illustrates the pH dependences of the $Ru^{IV}{=}O^{2+}/Ru^{III}{-}OH^{2+}$ and $Ru^{III}{-}OH^{2+}/Ru^{II}{-}OH_2^{2+}$ couples and, for comparison, the potentials for the couples $[Os(bpy)_3]^{3+/2+}$ ($E^{\circ\prime}$ = 0.81 V vs NHE) and $[Ru(NH_3)_5(py)]^{3+/2+}$ ($E^{\circ\prime}$ = 0.30 V).

The kinetics of reduction of *cis*-$[Ru^{III}(bpy)_2(py)(OH)]^{2+}$ and *cis*-$[Ru^{IV}(bpy)_2(py)(O)]^{2+}$ by $[Ru(NH_3)_5(py)]^{2+}$ were reported elsewhere.[23] In summary, reduction of *cis*-$[Ru^{IV}(bpy)_2(py)(O)]^{2+}$ by $[Ru^{II}(NH_3)_5(py)]^{2+}$ (at 22 °C, μ = 0.05 M, $k_{obs} = (8.71 \pm 0.02) \times 10^6$ M^{-1} s^{-1}) is independent of pH from pH 1.5 to 6 and independent of whether the electrolyte is perchlorate, triflate, or phosphate. Reduction of *cis*-$[Ru^{III}(bpy)_2(py)(OH)]^{2+}$ by $[Ru^{II}(NH_3)_5(py)]^{2+}$ is also independent of pH from pH 2.5 to 6 with $k_{obs} = (2.13 \pm 0.03) \times 10^7$ M^{-1} s^{-1} at 22 °C and μ = 0.05 M. The results are summarized in Table 1.

For reactions involving the $[Os(bpy)_3]^{2+/3+}$ couple, the direction of electron transfer was varied by changing the pH as indicated below:

$$cis\text{-}[Ru^{IV}(bpy)_2(py)(O)]^{2+} + H^+ + [Os^{II}(bpy)_3]^{2+} \underset{pH < 6.2}{\overset{pH > 6.2}{\rightleftharpoons}} cis\text{-}[Ru^{III}(bpy)_2(py)(OH)]^{2+} + [Os^{III}(bpy)_3]^{3+} \quad (2)$$

$$cis\text{-}[Ru^{III}(bpy)_2(py)(OH)]^{2+} + H^+ + [Os^{II}(bpy)_3]^{2+} \underset{pH < 4.5}{\overset{pH > 4.5}{\rightleftharpoons}} cis\text{-}[Ru^{II}(bpy)_2(py)(H_2O)]^{2+} + [Os^{III}(bpy)_3]^{3+} \quad (3)$$

Under many conditions, the kinetics of these reactions are complicated by contributions from the comproportionation equilibrium,[24,25]

$$cis\text{-}[Ru^{IV}(bpy)_2(py)(O)]^{2+} + cis\text{-}[Ru^{II}(bpy)_2(py)(H_2O)]^{2+} \underset{3 \times 10^3\ M^{-1}\ s^{-1}}{\overset{2.1 \times 10^5\ M^{-1}\ s^{-1}}{\rightleftharpoons}} cis\text{-}[Ru^{III}(bpy)_2(py)(OH)]^{2+} \quad (4)$$

Reduction of $Ru^{IV}{=}O^{2+}$ by $[Os^{II}(bpy)_3]^{2+}$ was investigated over the range 1 < pH < 8 and that of $Ru^{III}{-}OH^{2+}$ by $[Os^{II}(bpy)_3]^{2+}$ over the range 1 < pH < 5. The oxidations of $Ru^{II}{-}OH_2^{2+}$ and $Ru^{III}{-}OH^{2+}$ by $[Os^{III}(bpy)_3]^{3+}$ were studied from pH 4.5 to 8.3. The pH range was limited due to the instability of $[Os^{III}(bpy)_3]^{3+}$ in basic media (Experimental Section). Triple mixing techniques were employed to "pH jump" the $[Os^{III}(bpy)_3]^{3+}$ solutions immediately prior to mixing.

Table 1. Rate Constants for Reduction of *cis*-$[Ru^{IV}(bpy)_2(py)(O)]^{2+}$ and *cis*-$[Ru^{III}(bpy)_2(py)(OH)]^{2+}$ by $[Ru^{II}(NH_3)(py)]^{2+}$ at T = 22 °C, μ = 0.05 M in Aqueous Phosphate Buffers

$[Ru^{IV}{=}O]^{2+}$		
pH	$k \times 10^{-6}$ (M^{-1} s^{-1})	
1.43	8.65 ± 0.02	
2.66	8.75 ± 0.01	
4.50	8.82 ± 0.03	
6.02	8.61 ± 0.01	
2.60 (D_2O)	7.14 ± 0.07	$k_{H_2O}/k_{D_2O} = 1.23 \pm 0.02$
$[Ru^{III}{-}OH]^{2+}$		
pH	$k \times 10^{-7}$ (M^{-1} s^{-1})	
2.50	2.14 ± 0.03	
4.00	2.11 ± 0.05	
5.50	2.16 ± 0.02	

In Figures 2 and 3 are displayed representative absorbance−time curves illustrating the sometimes complex kinetic behavior observed in the reactions between $Ru^{IV}{=}O^{2+}$ or $Ru^{III}{-}OH^{2+}$ and $[Os^{II}(bpy)_3]^{2+}$ or $[Os^{III}(bpy)_3]^{3+}$, and the simple exponential behavior for the reaction between $Ru^{II}{-}OH_2^{2+}$ and $[Os^{III}(bpy)_3]^{3+}$.

It is possible to model the kinetic behavior in all pH and concentration domains by invoking two "square schemes" kinetically coupled with the comproportionation−disproportionation equilibrium in eq 4 (Scheme 3). The quantitative evaluation of rate constants and associated uncertainties involved fitting the results of over 500 separate kinetic runs which included an average of 8−12 experimental determinations performed under a given set of reaction conditions. The rate constants derived from this study are listed in Table 2. Only an upper limit of 3×10^3 M^{-1} s^{-1} could be estimated for k_{-3} in Scheme 3 because disproportionation, eq 4, dominates the mechanism of $Ru^{III}{-}OH^{2+}$ oxidation to $Ru^{IV}{=}O^{2+}$.

It is possible to check certain features of the proposed mechanism independently. Reduction of $Ru^{III}{-}OH^{2+}$ by $[Os^{II}(bpy)_3]^{2+}$, in acidic solution with $Ru^{III}{-}OH^{2+}$ in excess, gives $[Os^{III}(bpy)_3]^{3+}$ followed by slower re-equilibration of the disproportionation equilibrium in eq 4. At 630 nm, where $[Os^{II}(bpy)_3]^{2+}$ is the only appreciable light absorber, reduction of $Ru^{III}{-}OH^{2+}$ by $[Os^{II}(bpy)_3]^{2+}$ is the only reaction observed. Under these conditions the rate law becomes

$$-d[Os^{II}]/dt = k_{obs}[Ru^{III}_{tot}][Os^{II}]$$

with

$$k_{obs} = \{K^{III}_{a1}/([H^+] + K^{III}_{a1})\}\{(k_1[H^+]/K^{III}_{a1}) + k_2\} \quad (5)$$

In this equation, $[Ru^{III}_{tot}]$ is total Ru^{III} (=$[Ru^{III}{-}OH^{2+}]$ + $[Ru^{III}{-}OH_2^{3+}]$), K^{III}_{a1} is the first acid dissociation constant for $Ru^{III}{-}OH_2^{3+}$, and k_1 and k_2 are the rate constants for reduction of $Ru^{III}{-}OH_2^{3+}$ and $Ru^{III}{-}OH^{2+}$, respectively. A plot of k_{obs} vs pH is shown in Figure 4 and compared with the variation predicted by eq 5 with K^{III}_{a1} = 0.14, $k_1 = 5 \times 10^6$ M^{-1} s^{-1}, and $k_2 = 7.3 \times 10^1$ M^{-1} s^{-1}.

(23) Dovletoglou, A. Ph.D. Dissertation, The University of North Carolina, Chapel Hill, NC, 1992.

(24) Binstead, R. A.; Moyer, B. A.; Samuels, G. J.; Meyer, T. J. *J. Am. Chem. Soc.* **1981**, *103*, 2899−2901.

(25) Binstead, R. A.; Meyer, T. J. *J. Am. Chem. Soc.* **1987**, *109*, 3287−3297.

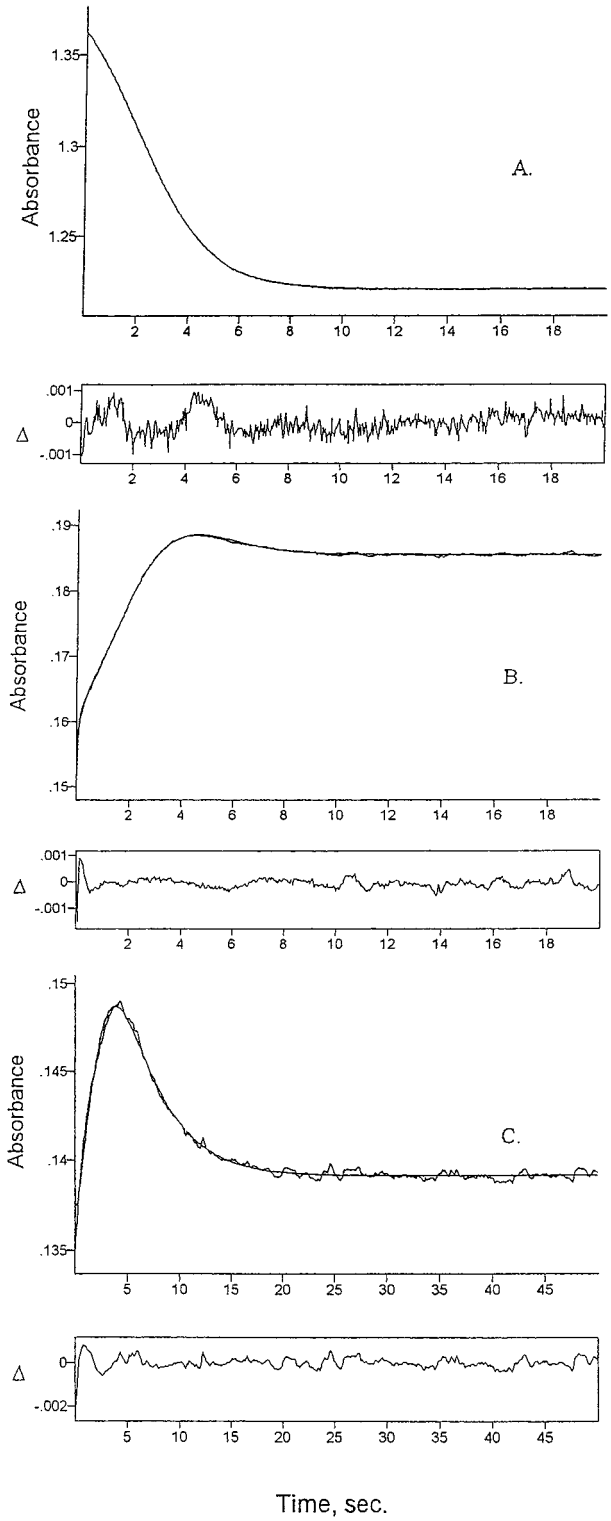

Figure 2. Single-wavelength absorbance−time traces, fit to the model in Scheme 4, and residuals (Δ), for the reaction between $Ru^{IV}{=}O^{2+}$ and $[Os^{II}(bpy)_3]^{2+}$ monitored at (A) 472 nm, pH 4.79, with $[Ru^{IV}{=}O^{2+}] = 1.78 \times 10^{-4}$ M and $[Os^{II}(bpy)_3{}^{2+}] = 1.82 \times 10^{-4}$ M; (B) 345 nm, pH 1.91, with $[Ru^{IV}{=}O^{2+}] = 1.17 \times 10^{-5}$ M and $[Os^{II}(bpy)_3{}^{2+}] = 9.20 \times 10^{-6}$ M; (C) 345 nm, pH 3.20, with $[Ru^{IV}{=}O^{2+}] = 1.12 \times 10^{-5}$ M and $[Os^{II}(bpy)_3{}^{2+}] = 1.46 \times 10^{-5}$ M. (The concentrations are those after mixing.)

To search for possible "remote" proton-coupled electron transfer, reduction of $Ru^{IV}{=}O^{2+}$ and $Ru^{III}{-}OH^{2+}$ by $[Os^{II}(bpy)_2(4\text{-}CO_2H\text{-}4'\text{-}CH_3bpy)]^{2+}$ and $[Os^{II}(bpy)_2(4\text{-}(CO_2{}^-)\text{-}4'\text{-}CH_3bpy)]^{+}$ was investigated from pH 2 to 4.5. The pK_a for $[Os^{II}(bpy)_2(4\text{-}CO_2H\text{-}4'\text{-}CH_3\text{-}bpy)]^{2+}$ was determined to be 3.8 ± 0.2 by pH titration.[26] From cyclic voltammetric measurements in phosphate buffers at 25 °C at pH 1.2, 2.6, 3.7, 4.5, 5.2, and 7.5, $E_{1/2}$ values for the protonated and deprotonated $Os^{III/II}$ couples are 860 ± 10 mV and 825 ± 10 mV (vs NHE, $\mu = 0.1$, scan rate = 100 mV/s). $E_{1/2} = 815$ mV for the $[Os(bpy)_3]^{3+/2+}$ couple under the same conditions.

The dominant reaction between $Ru^{IV}{=}O^{2+}$ and Os^{II} changes from

$$\textit{cis}\text{-}[Ru^{IV}(bpy)_2(py)(O)]^{2+} + [Os^{II}(bpy)_2(4\text{-}CO_2H\text{-}4'\text{-}CH_3bpy)]^{2+} \xrightarrow{k_4'} \textit{cis}\text{-}[Ru^{III}(bpy)_2(py)(OH)]^{2+} + [Os^{III}(bpy)_2(4\text{-}(CO_2{}^-)\text{-}4'\text{-}CH_3bpy)]^{2+} \quad (6)$$

at pH 2 to

$$\textit{cis}\text{-}[Ru^{IV}(bpy)_2(py)(O)]^{2+} + [Os^{II}(bpy)_2(4\text{-}(CO_2{}^-)\text{-}4'\text{-}CH_3bpy)]^{+} + H^+ \xrightarrow{k_4''} \textit{cis}\text{-}[Ru^{III}(bpy)_2(py)(OH)]^{2+} + [Os^{III}(bpy)_2(4\text{-}(CO_2{}^-)\text{-}4'\text{-}CH_3bpy)]^{2+} \quad (7)$$

at pH 4.5.[26]

The kinetics of these reactions, monitored at 445, 472, and 630 nm, could be fit to Scheme 3 with k_4', $k_4'' \approx (3.1 \pm 0.2) \times 10^3$ M^{-1} s^{-1} over the range $2 < pH < 4.5$. There was no sign of rate acceleration in acidic solution where the protonated form $[Os^{II}(bpy)_2(4\text{-}CO_2H\text{-}4'\text{-}CH_3bpy)]^{2+}$ dominates.

Similarly, the reaction between $Ru^{III}{-}OH^{2+}$ and Os^{II} changes from

$$\textit{cis}\text{-}[Ru^{III}(bpy)_2(py)(OH)]^{2+} + [Os^{II}(bpy)_2(4\text{-}CO_2H\text{-}4'\text{-}CH_3bpy)]^{2+} \xrightarrow{k_2'} \textit{cis}\text{-}[Ru^{II}(bpy)_2(py)(H_2O)]^{2+} + [Os^{III}(bpy)_2(4\text{-}(CO_2{}^-)\text{-}4'\text{-}CH_3bpy)]^{2+} \quad (8)$$

at pH 2 to

$$\textit{cis}\text{-}[Ru^{III}(bpy)_2(py)(OH)]^{2+} + [Os^{II}(bpy)_2(4\text{-}(CO_2\text{-})\text{-}4'\text{-}CH_3bpy)]^{+} + H^+ \xrightarrow{k_2''} \textit{cis}\text{-}[Ru^{II}(bpy)_2(py)(OH_2)]^{+} + [Os^{III}(bpy)_2(4\text{-}(CO_2{}^-)\text{-}4'\text{-}CH_3bpy)]^{2+} \quad (9)$$

at pH 4.5. The kinetics (monitored at 445, 472, and 630 nm) were fit to Scheme 3 with k_2', k_2'' varying from ~75 M^{-1} s^{-1} (pH 2.0) to ~70 M^{-1} s^{-1} (pH 4.5).

Discussion

The goal of this paper was to explore the kinetic and mechanistic consequences of proton-coupled electron transfer in reactions which are mechanistically constrained to be outer-sphere. As shown by the kinetic traces in Figures 2 and 3, one consequence is kinetic complexity. It occurs because electron

(26) Lebeau, E. L. Ph.D. Dissertation, The University of North Carolina, Chapel Hill, NC, 1997.

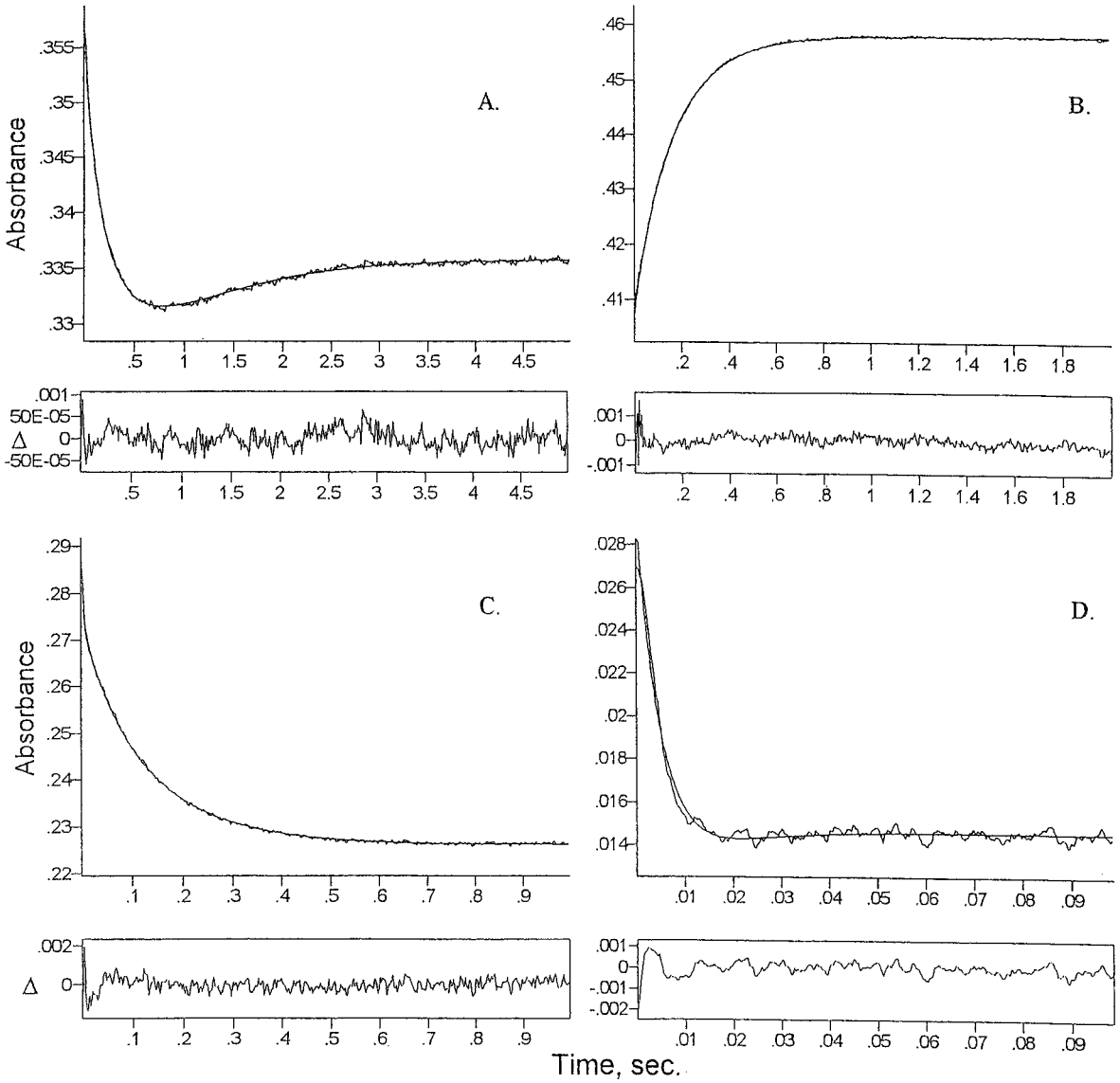

Figure 3. As in Figure 3 for (A) oxidation of Ru^{III}—OH^{2+} (5.13×10^{-5} M) by $[Os^{III}(bpy)_3]^{3+}$ (5.86×10^{-6} M) at 345 nm and pH 7.91; (B) oxidation of Ru^{II}—OH_2^{2+} (8.95×10^{-5} M) by $[Os^{III}(bpy)_3]^{3+}$ (8.33×10^{-6} M) at 400 nm and pH 6.28; (C) reduction of Ru^{III}—OH^{2+} (1.60×10^{-4} M) by $[Os^{II}(bpy)_3]^{2+}$ (1.77×10^{-5} M) at 472 nm and pH 3.68; (D) reduction of Ru^{III}—OH^{2+} (1.60×10^{-4} M) by $[Os^{II}(bpy)_3]^{2+}$ (1.77×10^{-5} M) at 630 nm and pH 3.68.

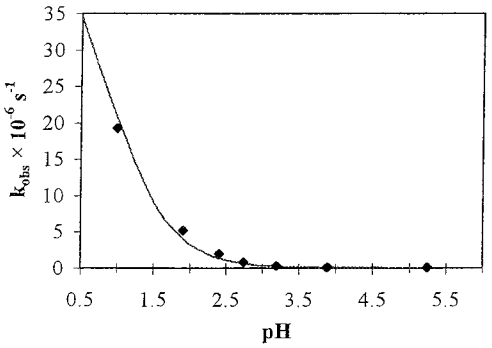

Figure 4. Experimental data (◆) and fit to eq 5 with $k_1 = 5 \times 10^6$ M^{-1} s^{-1}, $k_2 = 7.3 \times 10^1$ M^{-1} s^{-1}, $K^{III}_{a1} = 0.14$, and $[H^+] = 10^{-pH}$.

transfer is kinetically uncoupled from proton transfer. There is necessarily more than one step in the mechanism, and the interaction between them leads to complex kinetics.

The kinetic results can be satisfactorily modeled by invoking the coupled "square schemes" in Scheme 3 and the comproportionation equilibrium in eq 4. The results of this analysis reveal the existence of a series of kinetic nuances arising from mismatches between the proton requirements of the net reactions and the mechanisms by which they are forced to occur.

$$\underline{Ru^{III} + Os^{II} \rightleftharpoons Ru^{II} + Os^{III}}$$

$$cis\text{-}[Ru^{III}(bpy)_2(py)(OH)]^{2+} + H^+ + [Os^{II}(bpy)_3]^{2+} \rightarrow cis\text{-}[Ru^{II}(bpy)_2(py)(H_2O)]^{2+} + [Os^{III}(bpy)_3]^{3+}$$

Ru^{III} is distributed between Ru^{III}—OH^{2+} and Ru^{III}—OH_2^{3+} with $K^{III}_{a1} = 0.14$, eq 10.

$$cis\text{-}[Ru^{III}(bpy)_2(py)(H_2O)]^{2+} \rightleftharpoons cis\text{-}[Ru^{III}(bpy)_2(py)(OH)]^{+} + H^+ \quad (10)$$

Both forms participate in the oxidation of $[Os^{II}(bpy)_3]^{2+}$. For Ru^{III}—OH_2^{3+} the reaction is

Scheme 3

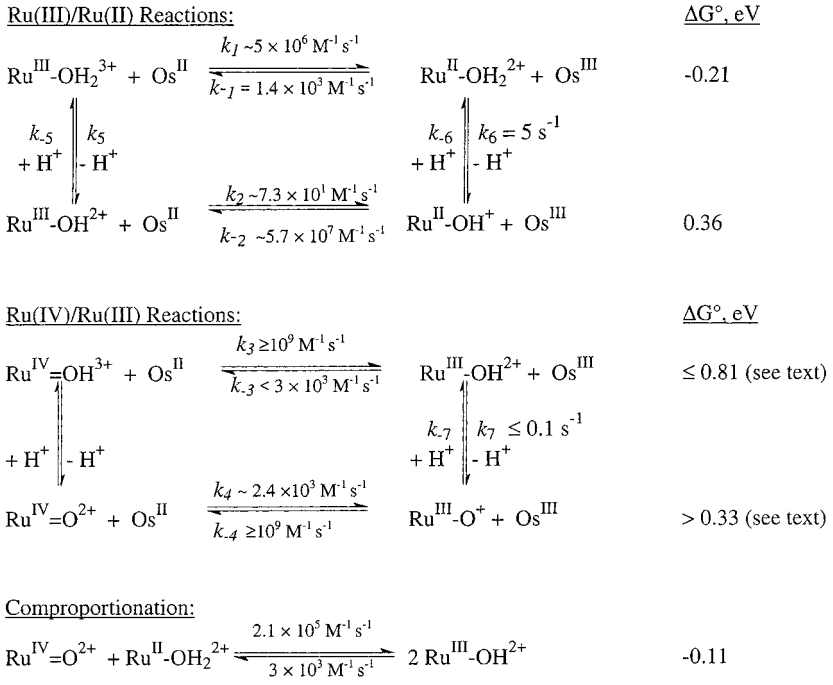

Table 2. Rate Constants for the Reactions in Scheme 3 at 25 °C and $\mu = 0.1$[a]

label	electron-transfer rate constant (M^{-1} s^{-1})	label	electron-transfer rate constant (M^{-1} s^{-1})
k_1	5×10^6	k_{-1}	1.4×10^3
k_2	$\sim 7.3 \times 10^1$	k_{-2}	5.7×10^7
k_3	$\leq 10^9$		
k_4	$\sim 2.4 \times 10^3$	k_{-4}	$\leq 10^9$

label	proton-transfer rate constant (s^{-1})	label	proton-transfer rate constant[b] (M^{-1} s^{-1})	comments: exptl pK_a	comments: lit. pK_a
k_5	1.5×10^{10}	k_{-5}	10^{11}	0.82	0.85[18,19]
k_6	5	k_{-6}	10^{11}	10.3	10.5[18,19]
k_7	≤0.1	k_{-7}	10^{11}	$k_7/k_{-7} < 10^{-14}$	>14

[a] There is no evidence for Ru^{IV}=OH^{3+} even in 1 M acid. [b] Taken as the diffusion-controlled limit for proton transfer.

$$cis\text{-}[Ru^{III}(bpy)_2(py)(H_2O)]^{3+} + [Os^{II}(bpy)_3]^{2+} \xrightarrow[\Delta G^\circ = -0.21\ eV]{k_1 \approx 5 \times 10^6\ M^{-1}\ s^{-1}} cis\text{-}[Ru^{II}(bpy)_2(py)(H_2O)]^{2+} + [Os^{III}(bpy)_3]^{3+} \quad (11)$$

With Ru^{III}—OH^{2+} as the oxidant, electron transfer is followed by acid−base equilibration.

$$cis\text{-}[Ru^{III}(bpy)_2(py)(OH)]^{2+} + [Os^{II}(bpy)_3]^{2+} \xrightarrow[\Delta G^\circ = +0.36\ eV]{k_2 \approx 7.3 \times 10^1\ M^{-1}\ s^{-1}} cis\text{-}[Ru^{II}(bpy)_2(py)(OH)]^{+} + [Os^{III}(bpy)_3]^{3+} \quad (12a)$$

$$cis\text{-}[Ru^{II}(bpy)_2(py)(H_2O)]^{2+} \rightleftharpoons cis\text{-}[Ru^{II}(bpy)_2(py)(OH)]^{+} + H^+$$

$$(k_6 = 0.5\ s^{-1},\ K^{II}_{a1} = 3.2 \times 10^{-10},\ pK_a = 10.5) \quad (12b)$$

The electron-transfer step in this case is uphill by 0.36 eV. The overall reaction is spontaneous because protonation following electron transfer provides the driving force with $\Delta G^\circ(eV) = 0.059$ pH.

For Ru^{III}—OH_2^{3+} as oxidant, electron transfer is favored by −0.21 eV. This pathway, eq 11, dominates in acidic solution. However, as the pH is increased, the concentration of Ru^{III}—OH_2^{3+} falls and oxidation by Ru^{III}—OH^{2+}, eq 12a, increases in importance. The distribution between pathways is given by $\{k_1[H^+]/([H^+] + K^{III}_{a1})\} + \{k_2 K^{III}_{a1}/([H^+] + K^{III}_{a1})\}$ or, with $[H^+] \ll K^{III}_{a1}$ (above pH 2), by $\{k_1[H^+]/K^{III}_{a1}\} + k_2$. These two pathways contribute equally by pH 4.9.

The distribution between pathways results in the pH dependence observed experimentally. It is true that the driving force for oxidation of $[Os(bpy)_3]^{2+}$ by Ru^{III} varies with pH, as shown in eq 13, but this is *not* the origin of the pH dependence.

$$\Delta G^\circ(eV) = -0.21 - 0.059 \log\{[H^+]/(K^{III}_{a1} + [H^+])\} \quad (13)$$

The disproportionation equilibrium in eq 4 complicates the kinetics under certain conditions. In acidic solution with Ru^{III} in excess, rapid reduction of Ru^{III} results in "kinetic overshoot" and overproduction of Ru^{II}—OH_2^{2+}. Under these conditions, electron transfer is followed by equilibration among Ru^{II}—OH_2^{2+}, Ru^{III}—OH^{2+}, and Ru^{IV}=O^{2+} which occurs on a slower time scale.

The enhanced rate constant for oxidation of $[Os^{II}(bpy)_3]^{2+}$ by Ru^{III}—OH_2^{3+} compared to Ru^{III}—OH^{2+} is predicted by the Marcus cross-reaction equation in the simplified form in eq 14.[4−6]

$$k_{12} \approx (k_{11} k_{22} K_{12})^{1/2} \quad (14)$$

In this equation, K_{12} is the equilibrium constant for the reaction, and k_{11} and k_{22} are the self-exchange rate constants for the Ru—$OH_2^{3+/2+}$ or Ru—$OH^{2+/+}$ and $[Os(bpy)_3]^{3+/2+}$ couples. If the k_{11} values are the same for the $Ru^{III/II}$ couples, their cross-reaction rate constants with $[Os^{II}(bpy)_3]^{2+}$ are related by $k_{12}'/k_{12} \approx (K_{12}/K_{12}')^{1/2}$. Based on K_{12} values derived from the redox

potential measurements, $k_{12}(Ru^{III}—OH_2^{3+})/k_{12}(Ru^{III}—OH^{2+}) = 6 \times 10^5$, which is close to the experimental ratio of $\sim 2 \times 10^4$.

For the oxidation of $[Ru^{II}(NH_3)_5(py)]^{2+}$, the $\Delta G°$ values are -0.71 eV for $Ru^{III}—OH_2^{3+}$ as reductant and -0.16 eV for $Ru^{III}—OH^{2+}$. There is no pH dependence from pH 6.2 to pH 2.5 with $k = (2.13 \pm 0.03) \times 10^7\ M^{-1}\ s^{-1}$, showing that electron transfer is dominated by $Ru^{III}—OH^{2+}$ as the oxidant. Since $Ru^{III}—OH_2^{3+}$ is a considerably stronger oxidant, it should dominate significantly at even lower pH with the distribution between pathways given by $(k_1[H^+]/Kk[Ru^{III}—OH_2^{3+}] = 10^9\ M^{-1}\ s^{-1}$, which is near the diffusion-controlled limit, and the two pathways would contribute equally at pH 2.5.

$$cis\text{-}[Ru^{II}(bpy)_2(py)(H_2O)]^{2+} + [Os^{III}(bpy)_3]^{3+} \rightarrow cis\text{-}[Ru^{III}(bpy)_2(py)(OH)]^{2+} + H^+ + [Os^{II}(bpy)_3]^{2+}$$

Above pH 4.5, the sense of the electron transfer is reversed, and Ru^{II} is oxidized by $[Os^{III}(bpy)_3]^{3+}$. The net reaction is distributed between the two pathways that are the microscopic reverse of eqs 11 and 12. In the first pathway, $[Os^{III}(bpy)_3]^{3+}$ is initially reduced by $Ru^{II}—OH_2^{2+}$,

$$cis\text{-}[Ru^{II}(bpy)_2(py)(H_2O)]^{2+} + [Os^{III}(bpy)_3]^{3+} \xrightarrow[\Delta G° = +0.21\ eV]{k_{-1} = 1.4 \times 10^3\ M^{-1}\ s^{-1}} cis\text{-}[Ru^{III}(bpy)_2(py)(H_2O)]^{3+} + [Os^{II}(bpy)_3]^{2+} \quad (15)$$

followed by proton equilibration at Ru^{III}, eq 12b. In the second pathway, the reductant is $Ru^{II}—OH^+$,

$$cis\text{-}[Ru^{II}(bpy)_2(py)(OH)]^{+} + [Os^{III}(bpy)_3]^{3+} \xrightarrow[\Delta G° = -0.36\ eV]{k_{-2} \approx 5.7 \times 10^7\ M^{-1}\ s^{-1}} cis\text{-}[Ru^{III}(bpy)_2(py)(OH)]^{2+} + [Os^{II}(bpy)_3]^{2+} \quad (16)$$

The generalized rate law in eq 17 can be derived by applying the steady-state approximation to $[Ru^{II}—OH^+]$ in Scheme 3 at pH < 9.5, where $Ru^{II}—OH_2^{2+}$ is the dominant form of Ru^{II}.

$$d[Os^{II}]/dt = k_{obs}[Os^{III}]\,[Ru^{II}—OH_2^{2+}] \quad (17a)$$

$$k_{obs} = [k_{-1} + \{k_{-2}k_6/(k_{-2}[Os^{III}] + k_{-6}[H^+])\}] \quad (17b)$$

In this expression, k_6 is the rate constant for proton dissociation from $cis\text{-}[Ru^{II}(bpy)_2(py)(H_2O)]^{2+}$.

Two important features emerge from this analysis: (1) The relative contributions of $Ru^{II}—OH_2^{2+}$ and $Ru^{II}—OH^+$ to electron transfer depend on both pH and $[Os^{III}]$. With $[Os^{III}] = 10^{-4}$ M and in pseudo-first-order excess, $Ru^{II}—OH_2^{2+}$ and $Ru^{II}—OH^+$ contribute equally to electron transfer at pH 5.7. Below this pH, $Ru^{II}—OH_2^{2+}$ dominates, while above it, $Ru^{II}—OH^+$ dominates. (2) Under certain conditions, the rate-limiting step is deprotonation of $Ru^{II}—OH_2^{2+}$, which occurs with $k_6 = 5\ s^{-1}$, eq 12b. At pH 7.2, deprotonation and electron transfer contribute equally as rate-limiting steps. Proton transfer is the slow step between pH 5.7 and 7.2.

Overview. There are important insights in this analysis: (1) If electron transfer is constrained to occur by an outer-sphere mechanism, the electron- and proton-transfer steps are uncoupled kinetically. They must occur in sequential steps that can lead to kinetic complexity. (2) There are parallel pathways for the aqua and hydroxo couples with the aqua couple, $Ru^{III}—OH_2^{3+/2+}$, more oxidizing and the hydroxo couple, $Ru—OH^{2+/+}$, more reducing. These reactions have different driving forces and undergo electron transfer with different rate constants. Their relative importance depends on the rate constants for the individual electron-transfer steps, the acid dissociation constant, and the pH. (3) The pH dependence originates in the distribution between acidic and basic forms of the reactant and *not in the driving force*. (4) There are domains where proton transfer from the reduced aqua form is rate limiting.

$$\underline{Ru^{IV} + Os^{II} \rightleftharpoons Ru^{III} + Os^{III}}$$
$$cis\text{-}[Ru^{IV}(bpy)_2(py)(O)]^{2+} + H^+ + [Os^{II}(bpy)_3]^{2+} \rightarrow cis\text{-}[Ru^{III}(bpy)_2(py)(OH)]^{2+} + [Os^{III}(bpy)_3]^{3+}$$

The mechanistic challenges arising from changes in proton content between oxidation states are exacerbated for the $Ru^{IV}=O^{2+}/Ru^{III}—OH^{2+}$ couple. For $d\pi^4$ $cis\text{-}[Ru^{IV}(bpy)_2(py)(OH)]^{3+}$, $pK_a < 0$ for the equilibrium $Ru^{IV}=OH^{3+} \rightleftharpoons Ru^{IV}=O^{2+} + H^+$. The $p\pi$ electron pairs on the O atom of the oxo group are highly mixed with $d\pi(Ru^{IV})$ orbitals and not readily available for bonding to protons. For $d\pi^5$ $cis\text{-}[Ru^{III}(bpy)_2(py)(OH)]^{2+}$, $pK_a > 14$. In this case, $p\pi(O) \rightarrow d\pi(Ru^{III})$ donation to the half-filled, highest $d\pi(Ru)$ orbital is greatly decreased, and the proton dramatically decreased in acidity compared to $Ru^{IV}=OH^{3+}$.

The difference in pK_a of >14 pH units has a dramatic effect on electron-transfer reactivity. Because of the inaccessibility of $Ru^{IV}=OH^{3+}$, the *only* pathway available for oxidation of $[Os^{II}(bpy)_3]^{2+}$ is initial electron transfer,[27]

$$cis\text{-}[Ru^{IV}(bpy)_2(py)(O)]^{2+} + [Os^{II}(bpy)_3]^{2+} \xrightarrow[\Delta G° > 0.36\ eV]{k_4 \approx 2.4 \times 10^3\ M^{-1}\ s^{-1}} cis\text{-}[Ru^{III}(bpy)_2(py)(O)]^{+} + [Os^{III}(bpy)_3]^{3+} \quad (18a)$$

followed by proton transfer,

$$cis\text{-}[Ru^{III}(bpy)_2(py)(OH)]^{2+} \xrightleftharpoons[(K^{III}_{a2} < 10^{-14})]{} cis\text{-}[Ru^{III}(bpy)_2(py)(O)]^{+} + H^+ \quad (18b)$$

The absence of a pH dependence rules out an important role for a pathway involving *simultaneous* electron transfer from $[Os^{II}(bpy)_3]^{2+}$ and proton transfer from a solvent molecule to $Ru^{IV}=O^{2+}$,

$$cis\text{-}[Ru^{IV}(bpy)_2(py)(O)]^{2+} + H_2O + [Os^{II}(bpy)_3]^{2+} \not\rightarrow cis\text{-}[Ru^{III}(bpy)_2(py)(OH)]^{2+} + OH^- + [Os^{III}(bpy)_3]^{3+} \quad (19)$$

This mechanism would introduce a pH dependence through its free energy change which varies as -0.059 V/pH unit, Figure 1.

The mechanism of reduction of $Ru^{IV}=O^{2+}$ by $[Ru^{II}(NH_3)_5(py)]^{2+}$ is the same. The rate law is first order in both $Ru^{IV}=O^{2+}$ and $[Ru^{II}(NH_3)_5(py)]^{2+}$ from pH 1.5 to 6. The rate constant, $k = (8.71 \pm 0.02) \times 10^6\ M^{-1}\ s^{-1}$, is greater than $k =$

(27) $\Delta G°$ for eq 18a can only be estimated. From the data in Figure 1, $E_{1/2}(Ru^{IV}=O^{2+}/Ru^{III}—OH^{2+})$ coincides with $E_{1/2}(Ru^{III}—OH^{2+}/Ru^{II}—OH^+)$ at pH ~12. As the pH is raised further, $E_{1/2}$ for the $Ru^{IV/III}$ couple falls below that for the $Ru^{III/II}$ couple and is no longer observable. $Ru^{III}—OH^{2+}$ becomes unstable with respect to disproportionation into $Ru^{IV}=O^{2+}$ and $Ru^{II}—OH^+$ past this pH, and only the two-electron $Ru^{IV}=O^{2+}/Ru^{II}OH^+$ couple is observed experimentally. From the crossover point in Figure 1, $E_{1/2}(Ru^{IV}=O^{2+}/Ru^{III}=O^+) < 0.45$ V, which gives $\Delta G° > 0.36$ eV for the electron-transfer step in eq 18a.

$(2.4 \pm 0.1) \times 10^3\ M^{-1}\ s^{-1}$ for reduction by $[Os^{II}(bpy)_3]^{2+}$. This is expected since $[Ru^{II}(NH_3)_5(py)]^{2+}$ is a stronger reductant by 0.51 eV.

Reduction of $Ru^{IV}{=}O^{2+}$ by $[Os^{II}(bpy)_3]^{2+}$ ($2.4 \times 10^3\ M^{-1}\ s^{-1}$) is more rapid than reduction by $Ru^{III}{-}OH^{2+}$ ($7.3 \times 10^1\ M^{-1}\ s^{-1}$), even though the driving force for this reaction is less. From the data in Figure 1, $E_{1/2}(Ru^{III}{-}OH^{2+}/Ru^{II}{-}OH^{+}) = 0.46$ and $E_{1/2}(Ru^{IV}{=}O^{2+}/Ru^{III}{=}O^{+})$ is less.[27]

Based on the relationship between free energy change and self-exchange in eq 14, the self-exchange rate constant for the $Ru^{IV}{=}O^{2+}/Ru^{III}{=}O^{+}$ couple must be greater than that for the $Ru^{III}{-}OH^{2+}/Ru^{II}{-}OH^{+}$ couple. This points to a lower intrinsic barrier to outer-sphere electron transfer for the $Ru^{IV}{=}O^{2+}/Ru^{III}{-}O^{+}$ couple. It also points to the important conclusion that $Ru^{IV}{=}O^{2+}$ is a *less* powerful one-electron oxidant than $Ru^{III}{-}OH^{2+}$ thermodynamically but has a lower reorganizational barrier to electron transfer.

$$cis\text{-}[Ru^{III}(bpy)_2(py)(OH)]^{2+} + [Os^{III}(bpy)_3]^{3+} \rightarrow cis\text{-}[Ru^{IV}(bpy)_2(py)(O)]^{2+} + [Os^{II}(bpy)_3]^{2+} + H^+$$

A further complication exists in the oxidation of $Ru^{III}{-}OH^{2+}$ to $Ru^{IV}{=}O^{2+}$ by $[Os^{III}(bpy)_3]^{3+}$, which is spontaneous above pH 6.2. The direct mechanism is the microscopic reverse of eq 18b with rate-limiting proton transfer,

$$cis\text{-}[Ru^{III}(bpy)_2(py)(OH)]^{2+} \underset{k_7}{\overset{k_7 \le 0.1\ s^{-1}}{\rightleftharpoons}} cis\text{-}[Ru^{III}(bpy)_2(py)(O)]^{+} + H^{+} \quad (20a)$$

followed by electron transfer,

$$cis\text{-}[Ru^{III}(bpy)_2(py)(O)]^{+} + [Os^{III}(bpy)_3]^{3+} \underset{\Delta G^\circ < 0.36\ eV}{\overset{k_4 \ge 10^9\ M^{-1}\ s^{-1}}{\rightleftharpoons}} cis\text{-}[Ru^{IV}(bpy)_2(py)(O)]^{2+} + [Os^{II}(bpy)_3]^{2+} \quad (20b)$$

The electron-transfer step is highly favored and occurs at or near the diffusion-controlled limit. The kinetically slow step is proton loss. The mechanism in eq 20 is sufficiently slow that it does not compete with a kinetic alternative, disproportionation,

$$2cis\text{-}[Ru^{III}(bpy)_2(py)(OH)]^{2+} \underset{2.1 \times 10^5\ M^{-1}\ s^{-1}}{\overset{3 \times 10^3\ M^{-1}\ s^{-1}}{\rightleftharpoons}} cis\text{-}[Ru^{IV}(bpy)_2(py)(O)]^{2+} + cis\text{-}[Ru^{II}(bpy)_2(py)(H_2O)]^{2+} \quad (21)$$

followed by oxidation of $cis\text{-}[Ru^{II}(bpy)_2(py)(H_2O)]^{2+}$ by $[Os^{III}(bpy)_3]^{3+}$. The limiting value of $k_7 < 0.1\ s^{-1}$ was obtained at low $Ru^{III}{-}OH^{2+}$ ($< 1 \times 10^{-6}$ M) where disproportionation is slow.

Electron transfer,

$$cis\text{-}[Ru^{III}(bpy)_2(py)(OH)]^{2+} + [Os^{III}(bpy)_3]^{3+} \xrightarrow{k_{-3} < 3 \times 10^3\ M^{-1}\ s^{-1}} cis\text{-}[Ru^{IV}(bpy)_2(py)(OH)]^{3+} + [Os^{II}(bpy)_3]^{2+} \quad (22)$$

followed by proton loss from $Ru^{IV}{=}OH^{3+}$, plays *no detectable role* under our conditions. $E_{1/2}$ for a related $Ru^{IV}{=}OH^{3+}/Ru^{III}{-}OH^{2+}$ couple is >1.6 V (vs SSCE). If relevant to the *cis*-$[Ru(bpy)_2(py)(OH)]^{3+/2+}$ couple, $\Delta G^\circ > 0.8$ eV for the electron-transfer reaction in eq 22.[28] The uphill nature of this reaction is a thermodynamic consequence of the high acidity of $Ru^{IV}{=}OH^{3+}$.

Overview. The results of the kinetic analysis for the Ru(IV/III) couple are highly revealing about the electron-transfer reactivity of metal oxo complexes: (1) The difference in pK_a of ≥ 14 between $Ru^{IV}{=}OH^{3+}$ and $Ru^{III}{-}OH^{2+}$ has a profound influence on electron-transfer reactivity. It causes $Ru^{IV}{=}OH^{3+}$ and $Ru^{III}{-}O^{+}$ to be inaccessible or present at low concentration at all but extreme pH values. (2) Oxidation of $Ru^{III}{-}OH^{2+}$ requires a powerful oxidant because $E_{1/2} > 1.6$ V for the $Ru^{IV}{=}OH^{3+}/Ru^{III}{-}OH^{2+}$ couple. $Ru^{IV}{=}O^{2+}$ is only a moderate oxidant, with $E_{1/2} < 0.45$ V for the $Ru^{IV}{=}O^{2+}/Ru^{III}{-}O^{+}$ couple. (3) The $Ru^{IV}{=}O^{2+}/Ru^{III}{-}O^{+}$ couple has a lower reorganizational energy than the $Ru^{III}{-}OH^{2+}/Ru^{II}{-}OH^{+}$ couple. (4) In the oxidation of $Ru^{III}{-}OH^{2+}$, proton transfer from $Ru^{III}{-}OH^{2+}$ is slow, with $k \leq 0.1\ s^{-1}$, and oxidation occurs by initial disproportionation.

Related Mechanisms. Proton-Coupled Electron Transfer. The difference in pK_a values inhibits outer-sphere Ru(IV/III) electron transfer and favors pathways more complex than single electron transfer.

One is *proton-coupled electron transfer*. An example appears in the comproportionation reaction between *cis*-$[Ru^{II}(bpy)_2(py)(H_2O)]^{2+}$ and *cis*-$[Ru^{IV}(bpy)_2(py)(O)]^{2+}$ in eq 4. This reaction is favored by 0.11 eV (2.5 kcal/mol) at 25 °C, $2 < pH < 9$, and occurs with $k = 2.1 \times 10^5\ M^{-1}\ s^{-1}$.[25] It is first order in $Ru^{IV}{=}O^{2+}$ and $Ru^{II}{-}OH_2^{2+}$, and there is a solvent kinetic isotope effect (k_{H_2O}/k_{D_2O}) = 16.1 at 25 °C. From the results of a mole fraction study, a single proton is involved.

The large kinetic isotope effect shows that there is significant coupling between the transferring electron and nuclear motion originating in an O−H bond in $Ru^{II}{-}OH_2^{2+}$. Electron transfer occurs from a dπ orbital in dπ^6(Ru^{II}) to a dπ orbital in dπ^4-(Ru^{IV}). The dπ^4(Ru^{IV}) orbitals are extensively mixed with the 2p$_\pi$(O) orbitals of the oxo group and are antibonding with regard to the Ru−O interaction. The aqua ligand in $Ru^{II}{-}OH_2^{2+}$ functions as a proton donor. The oxygen lone pairs on the oxo group in $Ru^{IV}{=}O^{2+}$ are proton acceptor sites which are increased in basicity by >14 pK_a units when electron transfer occurs. This combination of orbitals provides the electronic basis for proton-coupled electron transfer.[12,24,29]

Proton-coupled electron transfer is illustrated schematically in eq 23. H-bonding between an O−H bond of the aqua ligand and a lone pair on the oxo group probably initiates dπ(Ru^{IV})−dπ(Ru^{II}) orbital mixing and electronic coupling within an association complex of the reactants. Electron-vibrational coupling between the asymmetric $\nu(H_2O)$ stretching mode in $Ru^{II}{-}OH_2^{2+}$ and ν(Ru=O) in $Ru^{IV}{=}O^{2+}$ provides the quantum basis for coupled electron−proton motion.[30,31] The magnitude of the k_{H_2O}/k_{D_2O} kinetic isotope effect and its temperature dependence point to the importance of nuclear tunneling with electron transfer dominated by transitions from vibrational levels well below the classical intersection between potential curves. A critical parameter is the tunneling distance, the difference in the equilibrium coordinate for the transferring proton between the initial and final states.

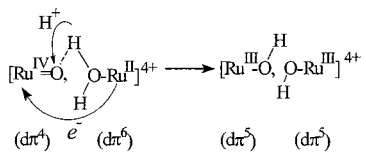

(23)

The change in pK_a between "$Ru^{IV}{=}OH^{3+}$" and $Ru^{III}{-}OH^{2+}$ plays an important role in this pathway. As electron transfer

(28) Trammell, S. A.; Wimbish, J. C.; Odobel, F.; Gallagher, L. A.; Narula, P. M., Meyer, T. J. *J. Am. Chem. Soc.* **1998**, *120*, 13248−13249.

(29) Binstead, R. A.; Stultz, L. K.; Meyer, T. J. *Inorg. Chem.* **1995**, *34*, 546−551.

Scheme 4

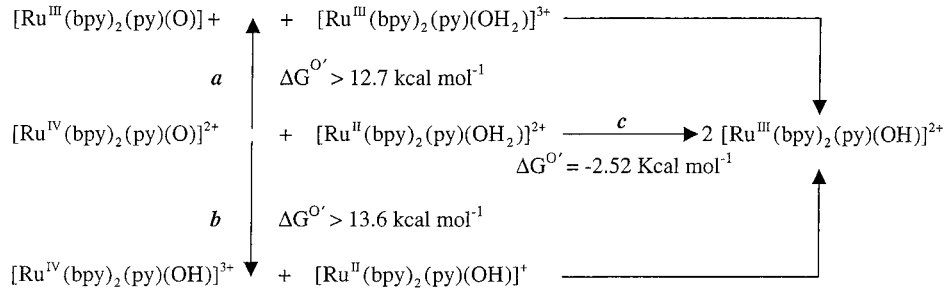

occurs, the largely inaccessible $p_\pi(O)$ lone pairs on the oxo group become highly basic and provide a coordination site for the addition of protons or other electrophiles. Defining the Ru−O bond to fall along the *z* axis in $Ru^{IV}{=}O^{2+}$, $d\pi$ (d_{xy},d_{yz}) mixing with $2p_\pi(O)$ (p_x,p_y) in $Ru^{IV}{=}O^{2+}$ results in the formation of π_1, π_2 and d_{xz}*, d_{yz}* ($d\pi$*) molecular orbitals. The $\pi_1$and π_2 orbitals are largely p_π in character and provide the basis for Ru−O multiple bonding. The $d\pi$* orbitals are the antibonding analogues and are largely d_{xz} and d_{yz} in character. Addition of an electron to one of the $d\pi$* orbitals results in a loss in π-bonding with concomitant formation of the σ(O−H) bond by a change in hybridization at the O atom.

The term "proton-coupled electron transfer" has been used in the literature in two ways. In one, it has been used to refer to net reactions such as eqs 2 and 3, where there is a change in proton content between reactants and products. As used here, the term has a mechanistic connotation. It refers to an electron-transfer pathway in which there is a *simultaneous* transfer of *both* protons and electrons from different sites in the molecule.[25,32]

When defined in this way, proton-coupled electron transfer is distinct from hydrogen atom transfer. In proton-coupled electron transfer, the electron and proton come from different orbitals in the donor—$d\pi(Ru^{II})$ and σ(O−H) in Ru^{II}—OH_2^{2+} in eq 23. In H atom transfer, both the electron and proton are transferred from the same orbital, such as a σ(C−H) bond in the oxidation of hydrocarbons.[33]

The difference between the two is put into perspective for the comproportionation reaction by comparing the proton-coupled electron-transfer mechanism in eq 23 with H atom transfer in eq 24. In this case, H atom transfer would produce the coordinated hydroxy radical intermediate, $[Ru^{II}(bpy)_2(py)(^{\bullet}OH)]^{2+}$, with electronic configuration $p_O{}^1d\pi^6$.

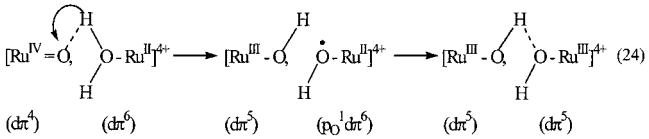

(24)

A $OH^- \rightarrow Ru^{III}$ charge-transfer band is observed in the spectrum of $[Ru^{III}(bpy)_2(py)(OH)]^{2+}$ at ~320 nm. Assuming a reorganizational energy of 1 eV for the transition would place the thermally equilibrated $p_O{}^1d\pi^6$ intermediate at >2 eV above the final product and inaccessible in the net reaction.

There are three reasonable electron-transfer pathways for the reaction between Ru^{II}—OH_2^{2+} and $Ru^{IV}{=}O^{2+}$, Scheme 4: (1) initial electron transfer followed by proton transfer (***a***); (2) initial proton transfer followed by electron transfer (***b***); and (3) proton-coupled electron transfer ***(c).*** Pathways ***a*** and ***b*** can be ruled out as significant contributors on energetic grounds. The $\Delta G°$ changes for the initial steps for both exceed the experimental free energies of activation, by >2.4 kcal/mol (***a***) and >3.2 kcal/mol (***b***), respectively.[24,25]

The kinetics study of the reaction between *cis*-$[Ru^{IV}(bpy)_2(py)(O)]^{2+}$ and $[Os^{II}(bpy)_2(4\text{-}CO_2H\text{-}4'\text{-}CH_3\text{-}bpy)]^{2+}$ was designed to search for a possible "remote" proton-coupled electron-transfer pathway in the reaction

$$\begin{aligned} &cis\text{-}[Ru^{IV}(bpy)_2(py)(O)]^{2+} + \\ &\quad [Os^{II}(bpy)_2(4\text{-}CO_2H\text{-}4'\text{-}CH_3bpy)]^{2+} \rightleftharpoons \\ &\quad cis\text{-}[Ru^{III}(bpy)_2(py)(OH)]^{2+} + \\ &\quad [Os^{III}(bpy)_2(4\text{-}(CO_2\text{-})\text{-}4'\text{-}CH_3bpy)]^{2+} \end{aligned}$$

In this pathway, electron-coupled proton transfer would occur from chemical sites that are well separated spatially and electronically. The $d\pi$ electron donor orbital at Os^{II} is well separated from the σ(O−H) proton donor orbital of the carboxylic acid group, eq 25. There is $d\pi$−π* mixing with the bpy ligand, but there is no significant basis for electronic coupling between electron and proton donor sites and there is no experimental evidence for this pathway.

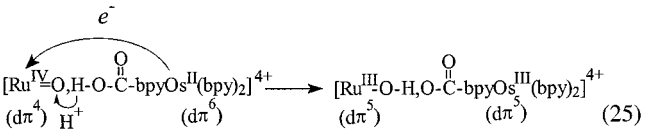

(25)

The rate constant for reduction of the acid complex ($k = 2.5 \times 10^3\ M^{-1}\ s^{-1}$) is comparable to that for reduction of $[Os^{II}(bpy)_3]^{2+}$ with $k = 2.4 \times 10^3\ M^{-1}\ s^{-1}$, and the $\Delta G°$ values are comparable (−0.36 eV for $[Os^{II}(bpy)_3]^{2+}$ and −0.31 eV for $[Os^{II}(bpy)_2(4\text{-}CO_2H\text{-}4'\text{-}CH_3bpy)]^{2+}$). We conclude that this reaction occurs dominantly by outer-sphere electron transfer,

$$\begin{aligned} &cis\text{-}[Ru^{IV}(bpy)_2(py)(O)]^{2+} + \\ &\quad [Os^{II}(bpy)_2(4\text{-}CO_2H\text{-}4'\text{-}CH_3bpy)]^{2+} \rightleftharpoons \\ &\quad cis\text{-}[Ru^{III}(bpy)_2(py)(O)]^{2+} + \\ &\quad [Os^{III}(bpy)_2(4\text{-}CO_2H\text{-}4'\text{-}CH_3bpy)]^{3+} \end{aligned} \quad (26)$$

followed by rapid protonation of Ru^{III}—O^+.

Electrochemistry. There are insights from the solution reactions for electron transfer at electrodes. In the absence of special surface effects, electron transfer must occur by the surface analogue of outer-sphere electron transfer.

In a voltammetric experiment, the direction of electron transfer can be varied by changing the electrode potential. If electron transfer is sufficiently rapid, diffusion is rate limiting.

(30) Cukier, R. I. *J. Phys. Chem.* **1996**, *100*, 15428−15443.
(31) Drukker, K.; DeLeeuw, S. W.; Hammes-Schiffer, S. *J. Phys. Chem.* **1998**, *108*, 6799−6808.
(32) Thorp, H. H. *Chemtracts: Inorg. Chem.* **1991**, *3*, 171−184.
(33) Mayer, J. M. *Acc. Chem. Res.* **1998**, *31*, 441−450.

The electrode response is thermodynamic, and the current−potential profile responds to changes in pH as predicted by the Nernst equation.

The same kinetic barriers to electron transfer exist at electrodes as in solution, and kinetic complexities also arise from changes in proton content. The $E_{1/2}$ value for the $Ru^{III}—OH_2^{3+}/Ru^{II}—OH_2^{2+}$ couple is 1.04 V, and that for the $Ru^{III}—OH^{2+}/Ru^{II}—OH_2^{2+}$ couple at pH 7 is 0.78 V. If oxidation of Ru^{II} to Ru^{III} at pH 7 occurs at 0.78 V and the mechanism is electron transfer from $Ru^{II}—OH_2^{2+}$ to the electrode to give $Ru^{III}—OH_2^{3+}$ rather than $Ru^{III}OH^{2+}$, $\Delta G° = +0.36$ eV for the electron-transfer step. This increases the electron-transfer barrier from $\Delta G^* = \lambda/4$ (at $\Delta G° = 0$) to $\Delta G^* = (\lambda + 0.36)^2/4\lambda$ (in eV), eq 1. The increased barrier slows electron transfer and can cause kinetic coupling to diffusion or even rate-limiting electron transfer and non-Nernstian behavior.[34]

McHatton and Anson have investigated the kinetics of electron transfer at rotating graphite disk electrodes as a function of pH for the $[Ru^{IV}(tpy)(bpy)(O)]^{2+}/[Ru^{III}(tpy)(bpy)(OH)]^{2+}$ and $[Ru^{III}(tpy)(bpy)(OH)]^{2+}/[Ru^{II}(tpy)(bpy)(H_2O)]^{2+}$ (tpy is 2,2′,2″-terpyridine) couples.[35] The rate constant for heterogeneous oxidation of $Ru^{II}—OH_2^{2+}$ to Ru^{III} (k_o) was pH dependent, reaching a minimum at pH ∼7 and increasing as the pH was increased or decreased.

The pH dependence of k_o is predicted by our analysis. The free energy change for oxidation of $Ru^{II}—OH_2^{2+}$ in acidic solution (in eV) is given by

$$\Delta G° = -[E°(Ru—OH_2^{3+/2+}) - E°(Ru^{III}—OH^{2+}/Ru^{II}—OH_2^{2+})] = 0.059(pH - pK^{III}_a) \quad (27)$$

From classical Marcus theory, the dependence of k_{ET} on $\Delta G°$ in eq 1 can be rewritten as

$$\ln k_{ET} = \ln k_{ET}(0) - (\Delta G°/2RT)\{1 + (\Delta G°/2\lambda)\} \quad (28)$$

In eq 28, $k_{ET}(0)$ is the electron-transfer rate constant at $\Delta G° = 0$, with the electrode potential at $E_{1/2}(Ru—OH_2^{3+/2+})$, assuming that $E_{1/2}$ is equal to the formal potential. This introduces the pH dependence in k_{ET} (and k_o) shown in eq 29. Based on this result, k_O increases as the pH is decreased because $E_{1/2}(Ru^{III}—OH^{2+})$ approaches $E_{1/2}(Ru^{III}—OH_2^{3+/2+})$.

$$\ln k_{ET} = \ln k_{ET}(0) - \{0.059(pH - pK^{III}_{a1})/2RT\}\{1 + [0.059(pH - pK^{III}_{a1})/2\lambda]\} \quad (29)$$

The increase in k_o as the pH is increased can be similarly explained. Oxidation of $Ru^{II}—OH_2^{2+}$ to $Ru^{III}—OH^{2+}$ by $[Os(bpy)_3]^{3+}$ above pH 7 is dominated kinetically by $Ru^{II}—OH^+$. From the analysis that led to eq 17, k_o is given by

$$k_O = k_{ET}(0)k_6/(k_{ET}(0) + k_{-6}[H^+]) \quad (30)$$

In eq 30, $k_{ET}(0)$ is the rate constant for $Ru^{II}—OH^+ \rightarrow Ru^{III}—OH^{2+}$ electron transfer at $\Delta G° = 0$ and k_6 the rate constant for proton loss from $Ru^{II}—OH_2^{2+}$ (Scheme 3). If proton loss is not rate limiting, this result predicts that k_o should increase with pH. Microscopically, this occurs because in the distribution between $Ru^{II}—OH_2^{2+}$ and $Ru^{II}—OH^+$ the latter is favored as the pH is increased.

McHatton and Anson also observed kinetic inhibition of the $[Ru^{IV}(tpy)(bpy)(O)]^{2+}/[Ru^{III}(tpy)(bpy)(OH)]^{2+}$ couple. In contrast to our results, they concluded that disproportionation played no role for this couple, at least at the electrode. The heterogeneous electron-transfer rate constant increased linearly with $[OH^-]$ in basic solution and linearly with $[H^+]$ in acid solution. They invoked pathways in which a terpyridine chelate arm was opened to give an intermediate that was more reactive toward electron transfer. There is no independent evidence that ring-opening occurs on the time scale of the electrochemical experiment. They also ruled out rate-limiting deprotonation of $Ru^{III}—OH^{2+}$ to give $Ru^{III}—O^+$ followed by electron transfer.

The apparent discrepancy between the solution and electrochemical results is not understood. There may be a role for catalytic surface effects arising from protonation−deprotonation and proton-coupled electron transfer. Previous work on carbon electrodes has shown this to be the case when Q-containing functional groups are introduced by oxidative pretreatment of the surface.[36−39]

Acknowledgment is made to the National Science Foundation under Grant CHE-9503738 for support of this research.

JA000517A

(34) Bard, A. J.; Faulkner, L. R. *Electrochemical Methods*; John Wiley: New York, 1980.
(35) McHatton, R. C.; Anson, F. C. *Inorg. Chem.* **1984**, *23*, 3935−3942.
(36) Cabaniss, G. E.; Diamantis, A. A.; Murphy, W. R.; Linton, R. W.; Meyer, T. J. *J. Am. Chem. Soc.* **1985**, *107*, 1845.
(37) Zen, J. M.; Jou, J. J.; Ilangovan, G. *Analysis* **1998**, *123* (6), 1345.
(38) Fernandez Abedul, M. T.; Costa Garcia, A. *J. Pharm. Biomed. Anal.* **1997**, *16* (1), 15.
(39) Huynh, M. H.; Meyer, T. J., in preparation.